UC San Diego
UC San Diego Previously Published Works

Title
Self-heating and electrical performance of carbon nanotube-enhanced cement composites

Permalink
https://escholarship.org/uc/item/83t226np

Authors
Lee, Heeyoung
Yu, Wonjun
Loh, Kenneth J
et al.

Publication Date
2020-07-01

DOI
10.1016/j.conbuildmat.2020.118838

Peer reviewed

Self-heating and electrical performance of carbon nanotube-enhanced cement composites

Heeyoung Lee, Ph.D.
Assistant Professor
Department of Civil Engineering, Chosun University
Telephone: 82-62-230-7087   Fax: 82-62-608-5216
E-mail: heeyoung0908@chosun.ac.kr

Wonjun Yu
Graduate Student
Kyung Hee University
Telephone: 82-31-201-3897   Fax: 82-31-202-8854
E-mail: 1208wonjun@gmail.com

Kenneth J Loh, Ph.D. (Co-corresponding Author)
Professor
University of California-San Diego, Department of Structural Engineering
Telephone: 1-858-822-0431   Fax: 1-858-822-0430
E-mail: kenloh@ucsd.edu

and

Wonseok Chung, Ph.D., P.E. (Corresponding Author)
Professor
Telephone: 82-31-201-2550   Fax: 82-31-202-8854
E-mail: wschung@khu.ac.kr

Department of Civil Engineering
College of Engineering
Kyung Hee University
1732 Deokyoung-Daero, Giheung-Gu
Yongin-Si, Gyeonggi-Do 17104

Republic of Korea

Self-heating and electrical performance of carbon nanotube-enhanced cement composites

Heeyoung Lee[a], Wonjun Yu[b], Kenneth J. Loh[c*], and Wonseok Chung[b*]

[a] Chosun University
[b] Kyung Hee University
[c] University of California-San Diego

* Corresponding Author: Department of Structural Engineering, University of California-San Diego, 9500 Gilman Drive MC 0085, La Jolla, CA 92093-0085, USA
Tel.: 1-858-822-0431
Fax: 1-858-822-0430
E-mail: kenloh@ucsd.edu

* Corresponding Author: Department of Civil Engineering, College of Engineering, Kyung Hee University, 1732 Deokyoung-Daero, Giheung-Gu, Yongin-Si, Gyeonggi-Do 17104
Tel.: 82-31-201-2550
Fax: 82-31-202-8854
E-mail: wschung@khu.ac.kr

Abstract

This work hypothesizes that mixing carbon nanotubes with cement improves the thermal and electrical properties of bulk cement composites. To test this, two different methods of combining cement and dispersed multi-walled carbon nanotubes (MWCNTs) were considered. In the first method, cement composites were produced by adding a dispersion of MWCNTs to cement. In the second, MWCNT-based thin films were spray-coated and combined with cement to produce cement composites. A third group of specimens was produced using both MWCNT dispersions and MWCNT film-coated. The experimental parameters considered were the mixing method, MWCNT concentrations, number of curing days, and voltages applied. Furthermore, field emission scanning electron microscopy revealed that the MWCNTs were evenly dispersed within the composites and formed a percolated network. Additionally, X-ray diffraction analysis confirmed that the products formed during hydration of the composites (i.e., C-H and C-S-H) were the same as those generated using ordinary mortar. Upon testing these mortar-based specimens, it was found that the cement composites formed using a combination of MWCNT dispersion and MWCNT-based films exhibited the highest heating performance and lowest electrical resistance. Finally, thermal imaging showed that increased MWCNT concentrations during specimen casting led to a corresponding increase in their surface temperature upon voltage application.

Keywords: cement composite, heating, microstructure, multi-walled carbon nanotube, nanocomposite, temperature performance

1. Introduction

Various technologies for designing and constructing large-scale concrete structures have been developed in recent years. Concrete materials are regularly used in various structures worldwide because of their excellent strength and durability. However, the use of concrete also leads to various problems related to the construction environment and global warming. Moreover, concrete structures can experience significant damage in the winter because of the black ice caused by snow. Thus, multifunctional concrete with improved strength and durability that can melt snow and ice must be developed to address the above-mentioned problems related to existing concrete structures.

Multifunctional concrete can potentially be synthesized by incorporating nanomaterials in existing construction materials [1-3]. Nanomaterials, which have particle sizes ranging from 0.1 to 100 nm, are attracting significant attention in various areas because of their high specific surface area per unit weight and excellent properties [4-7]. Nanomaterials can be mixed with construction materials based on ordinary cement to improve the mechanical, electrical, and thermal performances of the materials. Carbon nanotubes (CNTs), whose thermal conductivity and electrical conductivity are 7.5 and 100 times higher, respectively, than those of copper, have been mixed successfully with cement-based materials [8-12]. Further, there have been numerous studies on the mechanical and physical characteristics of cement composites formed using carbon nanomaterials to improve the strength, electrical conductivity, and heating performance [13-18].

Li and Zhao [13] fabricated specimens of ordinary mortar and its composites with multiwalled CNTs (MWCNTs) and carbon nanofibers (CNFs) and studied their compressive strengths. The results showed that the compressive strength of the composite with MWCNTs at 28 days was 19% higher than that of the composite consisting of ordinary mortar and CNFs. Further, the load transfer efficiency increased as more MWCNTs were added to the ordinary mortar because this resulted in a greater number of chemical bonds between the cement hydrates (C-S-H and calcium hydroxide). Chaipanich et al. [14] analyzed the compressive strength of cement mortar in which CNTs and fly ash had been mixed. The CNTs were added in concentrations of 0.5 and 1.0 wt% (cement weight). The results indicated that, for the same fly ash content, the compressive strength of the mortar increased with an increase in the CNT concentration because both the internal density and the extent of the CNT networks within the composite increased. Morsy et al. [15] fabricated mortar composites containing clay with nanosize particles and MWCNTs and studied their compressive strengths. The clay content was fixed at 6% of the cement weight and the MWCNT concentration was varied and composites with dimensions of 50 mm × 50 mm × 50 mm were fabricated. The composite with 0.02 wt% (by cement weight) MWCNTs exhibited a compressive strength 11% higher than that of ordinary mortar. On the other hand, the composite with 0.1 wt% MWCNT showed a lower compressive strength. Hamzaoui et al. [16] studied the mechanical properties of mortar and concrete containing CNTs, measuring the compressive strength of the composites containing CNTs in different concentrations. The compressive strength was the highest when CNTs were added in amounts of 0.01 and 0.003% by cement weight. The compressive strength increased with the addition of the CNTs because they served as bridges between the pores and cracks. Choi et al. [17] fabricated cement mortar by mixing dispersions of MWCNTs in distilled water and studied its compressive strength. It was found that the use of distilled water to form the MWCNT dispersions had little effect on the dispersibility of the CNTs. Kang et al. [18] studied the effects of the dispersibility of CNTs on the compressive and tensile strengths

of cement composites. CNTs were dispersed using surfactants, high-performance plasticizers, and an ultrasonic treatment. The results showed that the use of both ultrasonic treatment and high-performance plasticizers improved the compressive and tensile strengths by 10% as compared to the other dispersion methods.

As for studies on the electrical and heating performances of composites formed using nanomaterials, Nan et al. [19] elucidated the relationship between the CNT content and improvements in thermal conductivity for composites containing CNTs. Liu et al. [20] studied the thermal conductivity of nanofluids containing MWCNTs and found that the thermal conductivity of the nanofluids increased linearly with MWCNT concentration. Li et al. [21] used CNTs dispersed in sulfuric acid and nitric acid as well as unmixed CNTs to fabricate composite specimens with dimensions of 40 mm × 160 mm × 40 mm and measured their electrical resistances. Both the composite containing CNTs dispersed in sulfuric acid and nitric acid and that containing the unmixed CNTs exhibited significantly reduced electrical resistances, because the CNTs were uniformly dispersed and formed networks within the composites. Zhang and Li [22] studied the road deicing performances of MWCNT-containing cement composites. The results showed that a composite with a thermal conductivity of 2.83 W/m·K was formed when the MWCNTs were mixed in a concentration of 3% by the cement weight. Thus, it is possible to melt the ice formed on roads using MWCNT−cement composites. Kim et al. [23] studied the mechanical and electrical properties of cement composites containing silica fume and CNTs. It was found that the cement composites with low silica fume and CNT contents exhibited improved mechanical and electrical properties, owing to the decomposition of the aggregated CNTs into small clusters. Konst and Aza [24] analyzed the electrical properties and piezoresistive sensitivity of cement composites containing CNTs and CNFs. The cement composite formed using both CNTs and CNFs in concentrations of 0.1% by the cement weight. exhibited the highest piezoresistive sensitivity. Lee et al. [25] fabricated cement composites using MWCNTs and studied their electrical and thermal properties. The effects of the mixing method and MWCNT concentration were elucidated. The mixing methods used were forming a CNT coating on the fine aggregates and mixing the CNTs using a dispersion. The MWCNTs were added in concentrations of 0.125 and 0.25 wt% (by cement weight). The results showed that the composite formed using the former method exhibited better heating performance. Lee et al. [26] studied the heating performances of CNT-based cement composites. Different types of CNTs were used in varying concentrations, with the applied voltage also being a parameter. Specifically, SWCNTs and MWCNTs were used in combined concentrations of 0.0625 and 0.125 % (cement weight) while the voltages used were 50 and 100 V. The composite containing the MWCNTs and SWCNTs with a total concentration of 0.125% (by cement weight) exhibited better heating performance than that containing the CNTs in a total concentration of 0.0625 wt%. Thus, the heating performance increased with the total CNT concentration. Moreover, when a voltage of 100 V was supplied to the 0.125 wt% composite, its temperature rose by 70.6 °C. Thus, this composite exhibited better heating performance than the 0.12 wt% composite.

Finally, considering studies on nanomaterial-coated films, Hone et al. [27] fabricated an SWCNT film by filtration and desorption through a magnetic field and studied its heating performance. The SWCNT film exhibited a thermal conductivity of 200 W/m·K, which was similar to those of graphite and highly crystalline diamond. Haung et al. [28] studied the thermal conductivity of CNT films exhibiting different arrangements. For the same CNT concentration, the thermal conductivity was higher when the CNTs were arranged in the same direction. Kim et al. [29] fabricated CNT films with dimensions of 10 mm × 10 mm by

electrostatic spray deposition without using any binders and studied their electrical conductivity. The CNT films showed good electrical conductivities. In addition, the capacitance of the films was linearly proportional to their CNT concentration. Pham et al. [30] analyzed the electrical resistances of films of conductive CNTs and polymers under tensile strains. The results showed that the electrical resistance increased with an increase in the tensile strain owing to a decrease in the density of the conductive CNT network and an increase in the intertube distance. Park et al. [31] studied the heat diffusion performance of films of CNTs and polymers. The thermal diffusivity of the films was analyzed visually based on thermal images. Jang and Park [32] fabricated 25 mm × 25 mm films of composites with dispersed CNTs. The CNT concentration and film thickness were varied and the electrical conductivities and heating performances of the films were analyzed. The electrical resistance of the composite nanofilms decreased because the CNT networks became denser with an increase in the CNT concentration. Further, the electrical conductivity increased as the film thickness was increased. For temperatures of -5 to 5 °C, the films with low thicknesses exhibited greater temperature sensitivity.

In this study, the heating performances and electrical resistances of cement composites containing MWCNTs were analyzed. A widely employed method of incorporating MWCNTs into cement is to disperse the MWCNTs in a solution and then mix the solution with the cement [33-38]. In this study, however, both an MWCNT-containing solution and MWCNT-coated films were added to cement, and their effects on the heating performance and electrical resistance were measured. In particular, the effects of the mixing method used, MWCNT concentration, number of curing days, and applied voltage were investigated. As stated above, the mixing methods used included adding a solution containing the dispersed MWCNTs with ordinary mortar, adding MWCNT-coated films to ordinary mortar, and adding both the MWCNT solution and the MWCNT-coated films. The MWCNT concentrations used were 0.125, 0.25, and 0.5 wt% (by cement weight), and the mortar samples were cured for 7 and 28 days. The surface temperatures and thermal distributions of the composite samples were analyzed using thermal images. Finally, the internal microstructures of the MWCNT−cement composites were analyzed using field emission scanning electron microscopy (FE-SEM) and X-ray diffraction (XRD) analysis.

2. Experimental

As stated above, the investigated parameters were the MWCNT mixing method used, MWCNT concentration, number of curing days, and applied voltage. Table 1 lists the values of these parameters. The specimens were initially divided into groups based on the mixing method used. The specimens in Group#1 were fabricated by mixing a solution of dispersed MWCNTs with cement mortar. Those in Group#2 were fabricated by inserting MWCNT-coated films into cement mortar. Finally, those in Group#3 were fabricated by mixing a solution of dispersed MWCNTs with mortar and then inserting MWCNT-coated films into the mortar. The specimens were cured for 7 and 28 days, as these correspond to the compressive strength test criteria for cement mortar. Further, as mentioned previously, the MWCNT concentrations were 0.0, 0.125, 0.25, and 0.5 wt% (cement weight). Finally, direct current (DC) voltages of 10, 20, 30, and 60 V were used. Group # 2 and Group # 3 did not supply more than 30V because if the voltage is more than 30V, the film may be damaged.

The naming scheme used to label the various specimens is as follows. The first letter represents the mixing method. Here, "S" denotes the method in which a solution of dispersed MWCNTs was mixed in ordinary Portland cement while "F" refers to the method of adding MWCNT-coated films to mortar. Finally, "SF" denotes the method where both the solution of dispersed MWCNTs and the MWCNT-coated films were used. The second letter represents the number of curing days: "7D" means 7 days of curing while "28D" means 28 days of curing. Finally, the numerals "0.0", "0.125," "0.25," and "0.5" represent the total concentrations of the MWCNTs (wt% with respect to the cement weight). For example, ordinary Portland cement with 7 days of curing is expressed as 'S-7D-0.0'.

There are no standards available for determining the heating performance and electrical resistance of MWCNT−cement composites. Thus, specimens of the MWCNT−cement composites with dimensions of 50 mm × 50 mm × 50 mm, which are the standard specimen dimensions for testing the compressive strength test of cement mortar as per ASTM C 109, were formed (see Fig. 2) [15, 25, 26, 39]. The sand used was standard sand corresponding to the KSL ISO 679 standard. Additionally, ordinary Portland cement was used as the cement [40-42]. The used sand is KS L ISO 679 sand. This sand has a specific gravity of 2.6 – 2.67, uniformity of 1.0 – 1.93 and minimum dry unit weight of 13.8 – 14.38kN /m3. The used cement in this study is Class 1 Portland cement, as defined in KS L 5201. This cement is identical to ASTM Type I [43]. The MWCNT used in this paper is 99% pure and has an average diameter between 1 – 10nm and a length between 100nm – 1cm. The characteristics of MWCNTs are summarized in Table 2. Table 3 shows the mixing ratios for the various MWCNT−cement composites. The water/cement ratio was kept at 0.5 while the sand/cement ratio was set to 1:2.5 based on the weight. It should be noted that the MWCNT concentration is relative to the cement weight. The amounts of MWCNT in the cement composite for 0.125 wt%, 0.25 wt%, 0.5 wt% were 0.05 g, 0.1 g, 0.2 g, respectively, Furthermore, the amount of MWCNT present in the composite in which the MWCNT aqueous solution and the MWCNT-coated film were combined is the sum of the amount of MWCNT dispersed in the aqueous solution and the amount coated on the film. Figure 2 shows the process for fabricating the MWCNT−cement composites. To prepare the polymer films for coating with MWCNTs, first, a MWCNT dispersion was mixed in the copolymer polyacrylic acid for 2 hours under ultrasonication at 22 kHz. To prepare the MWCNT-coated films, polystyrene sulfonate and N-methylpyrrolidone solutions were mixed with this dispersion of MWCNTs [44-45]. Finally, a MWCNT dispersion was evenly coated on the transparent polymer films using an air compressor (Fig. 2(a).) The

amounts of the materials to be mixed were determined based on the mixing ratios. The cement and sand were subjected to dry mixing for 2 min to ensure homogeneous mixing (Fig. 2(b)). After the completion of the dry mixing process, plain water or the CNT dispersion was added to the dry mixture and mixed for 3 min, as shown in Fig. 2(c). After the mixing process, the mortar formed was compacted a total of 30 times to form specimens by dividing layers. For the composites formed using MWCNT-coated polymer films, the films were inserted after the mortar mixture had been poured (Fig. 2(d)). After the insertion of the films, the specimens were compacted again (Fig. 2(e)). In the case of composites containing the MWCNT films, Cu electrodes were attached to the films using silver epoxy. For the specimens formed using the MWCNT solution, Cu meshes were installed at intervals of 2.5 cm to apply a voltage. A thermocouple was installed at a depth of 2 cm in each specimen to measure the temperature at its center (Fig. 2(f)). Each specimen was demolded after being cured for 1 day at room temperature and then dried in an oven at 45°C [42]. The purpose of curing is to reduce the influence of moisture on the results of the experiment. The reason for using a 45 ° C oven is that according to KCS (Korean Construction Specification) 14 20 10, the temperature gradient should not exceed 15°C and not exceed 65°C per hour. In addition, a high temperature of 65°C or more may cause damage to the nanoparticles, so a 45°C oven was used.

As shown in Fig. 3(a), the voltage was applied using a DC power supply (EX-200). After connecting the (+) and (-) electrodes to the Cu meshes/electrodes installed in the MWCNT−cement composites, a voltage was applied using an insulating rubber plate. For each sample, the voltage was applied for 60 min. The internal temperature of each composite, which varied with the applied voltage, was measured by connecting the installed thermocouple to a data logger (TDS-303). The surface temperatures of the MWCNT−cement composites were analyzed based on thermal images, which allowed the maximum temperatures to be determined. To measure the electrical resistances of the MWCNT−cement composites, a digital multimeter (Keithley 2701) was used, as shown in Fig. 3(b). The (+) and (-) electrodes of the digital multimeter were connected to the Cu meshes/electrodes installed in the MWCNT−cement composites. The resistance in response to the applied voltage was measured with the digital multimeter for 60 min by connecting the multimeter to a computer. The internal microstructures of the MWCNT−cement composites were analyzed through FE-SEM and XRD analysis. FE-SEM uses an electron beam and an electron lens for microstructural analysis. This involves the magnification of objects based on the secondary and scattered electrons generated when the electron beam collides with the surface of the test specimen. XRD analysis allows for investigation of the structure and characteristics of an object based on the angle of diffraction of X-rays when they collide with the object.

3. Results and discussion

3.1. Heating tests and thermal imaging analysis

The effects of the mixing method, number of curing days, MWCNT concentration, and applied voltage on the heating performance were investigated. Figure 4(a) shows the maximum variations in temperature of the composites fabricated using the MWCNT solution after 7 days of curing. When a voltage of 60 V was applied to the specimens fabricated using the MWCNT solution, the temperature rose by 1.0 °C for the 0.0wt% composites, by 1.3 °C for the 0.125wt% composites, by 1.8 °C for the 0.25 wt% composites, and by 19.8 °C for the 0.5 wt% composites. Thus, the temperature increase for the 0.5 wt% composites was 19.8 times higher than that for

7

the composites with 0.0 wt% MWCNTs, which was the lowest concentration. Hence, it can be concluded that the temperature increased with MWCNT concentration. Figure 4(b) shows the maximum temperature variations at the centers of the composites formed using the MWCNT films after 7 days of curing. On the other hand, when the voltage applied was 30 V, for the composites fabricated using the MWCNT films, the temperature increase was 0.7 °C for the 0.125 wt% composites, 9.5 °C for the 0.25 wt% composites, and 37.2 °C for the 0.5 wt% composites. Thus, the 0.5 wt% composites with the MWCNT films exhibited a temperature increase that was 7.2 times higher than that for the MWCNT-solution composites with the same MWCNT concentration at 60 V. Therefore, the composites with the inserted MWCNT films exhibited relatively higher temperatures even at a lower voltage (30 V). Figure 4(c) shows the maximum variations in the temperature of the composites fabricated using both the MWCNT solution and the MWCNT films after 7 days of curing. When a voltage of 30 V was applied to the composites fabricated using both the MWCNT solution and the MWCNT films, the temperature increase was 0.8 °C for the 0.125 wt% composites, 10.9 °C for the 0.25 wt% composites, and 77.5 °C for the 0.5 wt% composites. Thus, for a voltage of 30 V, the 0.5 wt% composites formed using a combination of the MWCNT solution and the MWCNT films exhibited a temperature increase 13.9 times higher than that of the composites that had the same MWCNT concentration but were fabricated using the MWCNT solution and 2.1 times higher than that of the composites that had the same MWCNT concentration but were fabricated using MWCNT films. Hence, use of a combination of the MWCNT solution and the MWCNT films resulted in improved heating performance. This is because the aforementioned combination generates heat when current flows through the film. Furthermore, the cement composites consisting of the MWCNT solution have excellent thermal conductivity; therefore, the heat generated from the MWCNT film is uniformly distributed throughout the aforementioned combination. For this reason, the heat performance of the composite fabricated using the MWCNT solution and film combination was the most optimal.

Figure 4(d) shows the temperature variations at the centers of the MWCNT−cement composites formed using the MWCNT solution after 28 days of curing. For an applied voltage of 60 V, the temperature of the composites fabricated using the MWCNT solution increased by 0.5 °C for the 0.0 wt% specimen, by 0.6 °C for the 0.125 wt% specimen, by 0.9 °C for the 0.25 wt% specimen, and by 16.8 °C for the 0.5 wt% specimen. The temperature of the 0.125 wt% specimen cured for 28 days was 0.7 °C lower than that of the corresponding 0.125 wt% specimen cured for 7 days. Similarly, the temperature of the 0.5 wt% specimen cured for 28 days was 3 °C lower than the corresponding specimen cured for 7 days. Figure 4(e) shows the heating performance graph of the MWCNT−cement composites fabricated by inserting MWCNT films for different voltages and MWCNT concentrations. When a voltage of 30 V was applied, the temperature rose by 0.9 °C for the 0.125 wt% specimen, by 3.7 °C for the 0.25 wt% specimen, and by 36.1 °C for the 0.5 wt% specimen. The heating performances of the specimens cured for 28 days were slightly lower compared to those of the corresponding ones cured for 7 days. Figure 4(f) shows the heating performance graph of the MWCNT−cement composites fabricated using both the MWCNT solution and the MWCNT films. For a voltage of 30 V, the temperature increased by 0.8 °C for the 0.125 wt% specimen, by 5.1 °C for the 0.25 wt% specimen, and by 76.4 °C for the 0.5 wt% specimen. Hence, both the method of using the MWCNT solution and the MWCNT films and curing for 7 days resulted in excellent heating performances. Moreover, the specimens in Group#3 also showed slightly lower heating performances after 28 days of curing. The difference in temperature increase due to the

8

difference in the number of curing days was 0 °C for the 0.125 wt% specimens, 5.8 °C for the 0.25 wt% specimens (this was the largest difference), and 1.1 °C for the 0.5 wt% specimens. This trend can be attributed to the fact that the hydration reaction did not increase the temperature significantly, owing to the effects of moisture, when the MWCNT−cement composites were cured for 7 days [47].

Table 4 lists the temperatures of the MWCNT−cement composites according to the various parameters. The highest temperatures were 77.5 °C for SF-7D-0.5 after 7 days of curing and 76.4 °C for SF-28D-0.5 after 28 days of curing. This is because more CNT networks were formed in these specimens, as the CNTs were evenly dispersed not only in the MWCNT-coated films but also within the composites. The temperatures of the composites increased with the MWCNT concentration. Moreover, as the number of curing days was increased, the increase in the temperature decreased; this was because of the reduced effect of the moisture present in the samples. However, the temperature increases after 7 and 28 days of curing were similar.

Figure 5 shows the thermal images of the MWCNT−cement composites after 28 days of curing. As shown in Figure 5, the surface temperature of the cement composite is calculated by adding the initial internal temperature of the composite and the temperature change. For example, SF-28D-0.5 has an initial internal temperature of 25.1 °C and a temperature change of 76.4 °C. Thus, the SF-28D-0.5 surface temperature was calculated to be 101.5 °C. Figures 5 (a) and 5(b) show the thermal images of the composites fabricated using the MWCNT solution when voltages of 30 and 60 V, respectively, were applied. At 60 V, the surface temperatures of S-28D-0.125, S-28D-0.25, and S-28D-0.5 were 20.7, 21.1, and 42.4°C, respectively. Thus, for a voltage of 60 V, the surface temperatures of the MWCNT−cement composites increased by up to 14.2 °C compared to those for 30 V.

For the same applied voltage, the surface temperature increased with the MWCNT concentration, resulting in clear thermal images. Moreover, in the case of the composites fabricated using the MWCNT solution, heating occurred primarily between the electrodes connected to the voltage supply. This was because current has a tendency to flow along the shortest distance; thus, the heat generated was distributed mainly between the electrodes. Figure 5(c) shows the thermal images of the composites fabricated by inserting MWCNT films. When the voltage was 30 V, the highest surface temperature was 60.5 °C and was observed in the case of F-28D-0.5. However, for the same voltage, the temperatures of the cement composites fabricated by inserting MWCNT films were 35.1 °C higher than those of the composites fabricated using the MWCNT solution. Sample OF-28D-0.125 exhibited a temperature of 21.1 °C, with its thermal image showing the insignificant temperature. Further, its temperature was 0.4 °C higher than that of S-28D-0.125 and thus not significantly different. The temperature of F-28D-0.25 was 24.2°C, and its thermal image clearly indicated an increase in the surface temperature as compared to that of S-28D-0.25. For the composites formed using the MWCNT films, the temperature change occurred from the center, where the films were inserted. This was because the MWCNTs were concentrated on the film surfaces. Figure 5(d) shows the thermal images of the composites fabricated using both the MWCNT solution and the MWCNT films. The surface temperature of SF-28D-0.5 was 101.5 °C, which was the highest after 28 days of curing.

The samples fabricated using both the solution and the films having MWCNT concentrations of 0.25 wt% and 0.5 wt% exhibited higher temperatures than those of the composites formed using only the MWCNT films. The heating performance of the former was better because in their case, the MWCNTs were evenly dispersed in the films; therefore, the composites, with

9

CNT networks forming throughout the specimens.

Figure 6 shows the temperature graphs of the MWCNT−cement composites over time. Figures 6 (a) and 6(b) show the temperature graphs of the composites fabricated using the MWCNT solution over time. The samples with 0.125 wt% MWCNTs exhibited relatively small temperature increases than those with 0.25 and 0.5 wt% MWCNTs. For the composites fabricated using the MWCNT solution, the temperature gradient increased with the MWCNT concentration, with the temperatures plateauing once the highest temperatures had been reached. Moreover, the temperature gradient after 7 days of curing was higher than that after 28 days. Thus, it can be concluded that the temperature gradient was relatively higher because the current flowed well in the composites owing to the effects of the moisture present within them. Figures 6 (c) and 6(d) show the temperature increase graphs over time of the composites fabricated using the MWCNT films and cured for 7 and 28 days, respectively. The temperature gradients and temperatures varied depending on the mixing method used. Except for F-0.5-30V at 7 and 28 days, the temperatures remained constant over time as with the method of mixing solution. For F-0.5-30V, the temperature increased initially, reaching the maximum value, and then decreased over time. Figures 6(e) and 6(f) show the temperature graphs over time for the composites fabricated using both the MWCNT solution and the MWCNT films. The temperature gradients were relatively higher than those of the specimens formed using the MWCNT solution as well as those formed using the MWCNT films. This suggests that the temperatures and thermal diffusivities increased in the former case because the MWCNTs dispersed in the solution and films formed CNT networks together. For SF-0.5-30V as well, the temperature first increased, reaching the maximum value, and then decreased. As with the ordinary mortar, when a voltage of 30 V or higher was applied to the composites formed using the MWCNT films, the inserted films were damaged, as shown in Figure 7. As a result, the networks of the dispersed MWCNTs were destroyed, resulting in a decrease in the heating performance. Therefore, care should be taken when applying high voltages (30V or higher), as the MWCNT films can be damaged in such cases.

3.2. Electrical resistance measurements

Figure 8(a) shows the resistance graphs of the MWCNT−cement composites formed using the MWCNT solution after 7 days of curing. In the case of the composites fabricated using the MWCNT solution, the resistance of the 0.0 wt% specimen was 972 kΩ, 0.125 wt% specimen was 52.8 kΩ and that of the 0.25 wt% specimen was 20.72 kΩ. Thus, the resistance of the latter was 46.9 times lower than 0.0 wt% specimen. Further, the resistance of the 0.5 wt% specimen was 0.9 kΩ, which was 59 times lower than that of the 0.125 wt% specimen (Fig. 8(a)). These results indicate that the electrical resistance reduced as the MWCNT concentration was increased, because the CNTs formed denser networks as their content was increased[46]. Figure 8(b) shows the resistance graphs of the MWCNT−cement composites fabricated using the MWCNT films after 7 days of curing. In the case of the composites formed using the MWCNT films, the resistance was 88.4 kΩ for the 0.125 wt% specimen, 0.74 kΩ for the 0.25 wt% specimen, and 0.075 kΩ for the 0.55 wt% specimen (Fig. 10(b)). Further, the resistances of the 0.25 wt% and 0.5 wt% specimens were 28% and 12% lower, respectively, compared to those of the composites fabricated using the MWCNT solution—the 0.125 wt% specimen was an exception here. Figure 8(c) shows the electrical resistances of the MWCNT−cement composites fabricated using both the MWCNT solution and the MWCNT films. The electrical resistance was 82.9 kΩ for the 0.125 wt% specimen, 0.71 kΩ for the 0.25 wt% specimen, and

0.05 kΩ for the 0.5 wt% specimen. These results were similar to those for the corresponding specimens fabricated using the MWCNT films. This suggests that the differences in electrical resistance of the corresponding specimens from the two groups were insignificant because the electrodes of the MWCNT films were integrated with the films. The electrical resistance experiments measured the resistance caused by a fine current supply. Since the CNT-films used in Group # 2 and Group # 3 were integrated with the copper electrode, the difference in resistance due to small currents accurately measures the resistance of CNTs dispersed in the film. Therefore, the differences in resistance of CNT-films coated with the same concentration are considered to be insignificant.

Figure 8(d) shows the resistance graphs for the composites produced using the MWCNT solution after 28 days of curing. The resistance of the 0.0 wt% specimen was 980 kΩ, which was the largest resistance increase for the composites formed using the MWCNT solution after 28 days of curing. The resistance of the 0.125 wt% specimen was 62.1 kΩ, which was 9.3 kΩ higher compared to that after 7 days of curing. The resistance of the 0.25 wt% specimen increased by 5.08 kΩ to 25.8 kΩ while the resistance of the 0.5 wt% specimen increased by 0.08 kΩ to 0.98 kΩ. With an increase in the curing duration, the electrical resistance of the specimens increased but their temperature upon the application of a voltage decreased slightly. Figure 8(e) shows the resistance graphs for the composites produced using the MWCNT films after 28 days of curing. The resistance was 98.9 kΩ for the 0.125 wt% specimen, 3.2 kΩ for the 0.25 wt% specimen, and 0.1 kΩ for the 0.5 wt% specimen. For the 0.5 wt% specimen, the resistance was higher by 0.025 kΩ compared to that after 7 days of curing. Figure 8(f) shows the resistance graphs of the composites fabricated using both the MWCNT solution and the MWCNT films after 28 days of curing. The resistance of the 0.125 wt% specimen was 98.5 kΩ and higher by 0.4 kΩ than that of OF-28D-0.125. The resistance of the 0.25 wt% specimen was 2.91 kΩ and higher by 0.29 kΩ than that of F-28D-0.25. Finally, the resistance of the 0.5 wt% specimen was 0.067 kΩ. These resistance values were lower than those of the corresponding composites fabricated using the MWCNT films after 7 days of curing.

Table 5 lists the electrical resistances of the various MWCNT−cement composites. Of the various composites formed using the MWCNT solution, S-7D-0.5 exhibited the lowest resistance at 0.9 kΩ. As for the composites formed using the MWCNT films, OF-7D-0.5 showed a resistance of 0.075 kΩ, which was 12 times lower than that of S-7D-0.5. Finally, in the case of the composites fabricated using both the MWCNT solution and the MWCNT films, SF-7D-0.5 exhibited a resistance of 0.05 kΩ, which was the lowest of all the composites. The resistance decreased as the MWCNT concentration was increased because the presence of a greater number of conductive MWCNTs resulted in denser CNT networks. Further, as the number of curing days was increased, the resistance increased slightly because the hydration process of the cement composites occurred to completion. However, the differences in resistance corresponding to the different curing durations were insignificant[38].

3.3. Microstructural analysis

Figure 9 shows the XRD patterns of the composites formed using the MWCNT solution. Peaks were observed between 2θ values of 26º and 29º for the pure mortar sample as well as the 0.125, 0.25, and 0.5 wt% samples. This suggested that portlandite (C-H), a hydrate generated during the hydration reaction, was formed in the case of every sample. The peak at 38°, which was observed for every specimen, is attributable to calcium silicate hydrates (C-S-H), which significantly affect the strength. These results indicated that in each MWCNT−cement composite, the same hydration process occurred and that the same hydration

486   products were generated as those in ordinary mortar.

487   Figure 10 shows FE-SEM images of the MWCNT−cement composites. The red crosses in
488 the images represent MWCNTs. Figure 10(a) shows a microstructural image of the composite
489 formed using the 0.5 wt% MWCNT solution. The image confirmed that MWCNTs were evenly
490 dispersed in the composite and that CNT networks were formed in it, as the cement hydrates
491 and MWCNTs were connected. The formation of these CNT networks appears to have
492 improved the heating performance and electrical conductivity of the composites. Figure 10(b)
493 shows a microstructural image of a film damaged by a voltage of 30 V. No CNT networks can
494 be seen in this film, as the MWCNTs connected on the film surface became disconnected after
495 the application of the voltage. This was the reason for the poorer heating performance and
496 higher electrical resistance of the composites with the MWCNT-coated films. Figure 10(c)
497 shows a microstructural image of an undamaged MWCNT-coated film. A number of red
498 crosses can be seen distributed on the surface of the film. This indicated that the MWCNTs did
499 not aggregate and remained concentrated on the surface of the film, forming CNT networks.

500

501

4. Conclusions

In this study, MWCNT–cement composites were fabricated using MWCNTs, which were mixed in cement using three different methods. The heating performances and electrical resistances of the fabricated composites were also investigated. Based on the experimental results, the performances of the MWCNT–cement composites were analyzed, and the following conclusions were drawn:

1. With respect to the methods used for incorporating MWCNTs, the composites formed by inserting MWCNT-coated films in a mortar exhibited better heating performance than those formed by the mixing of a MWCNT-dispersed solution in the cement. The highest temperature increase at 30 V was 37.2 °C and was seen in the case of F-7D-0.5, while that at 60 V was 19.8 °C and was seen in the case of S-7D-0.5. The heating performance of the composites formed using the MWCNT films was 1.9 times higher than that of the composites formed using the MWCNT solution. This result suggested that the increase in temperature per unit area was higher in the former case because the MWCNTs were concentrated on the film surfaces.

2. In the case of the composites fabricated using both the MWCNT solution and the MWCNT films, the highest temperature increase was 77.5 °C and was observed in the case of SF-7D-0.5. This sample also exhibited the lowest electrical resistance at 0.05 kΩ. Thus, use of both the MWCNT solution and the MWCNT films is the most suitable method for improving the heating performance and electrical conductivity. This is because more CNT networks were formed in these specimens, as the CNTs were evenly dispersed not only in the MWCNT-coated films but also within the composites themselves.

3. The higher the MWCNT concentration was, the higher the heating performance and the lower the electrical resistance became. This is because the presence of a greater number of conductive MWCNTs meant that more CNT networks were formed in the cement composites.

4. As the number of curing days was increased, the heating performance decreased slightly and so did the electrical resistance. After 7 days of curing, the heating performance increased relatively and so did the electrical resistance owing to the effects of the moisture present within the composites. Future research will be conducted to study the heating and resistive performance of long-term curing over 28 days of curing of MWCNT-cement composites.

5. The XRD analysis results confirmed that portlandite (C-H) and calcium silicate hydrates (C-S-H) were also formed in the MWCNT–cement composites in the same manner as in ordinary mortar during the hydration process. Thus, it can be concluded that the same hydration processes also occurred in cement composites containing MWCNTs. The FE-SEM results confirmed the formation of CNT networks on the surfaces of the MWCNT films, which improved the heating performance and reduced the electrical resistance. In the case of the MWCNT film damaged by the application of a high voltage, the heating performance decreased and the electrical resistance increased owing to breakage of the CNT networks.

13

References

[1] L. Raki, J. Beaudoin, R. Alizadeh, J. Makar, T. Sato, Cement and concrete nanoscience and nanotechnology, Mater. 3 (2010) 918–942.

[2] F. Sanchez, K. Sobolev, Nanotechnology in concrete–a review, Constr. Build. Mater. 24 (2010) 2060–2071.

[3] M.J. Hanus, A.T. Harris, Nanotechnology innovations for the construction industry, Prog. Materi. Sci. 58 (2013) 1056–1102.

[4] Z. Fan, J. Chen, M. Wang, K. Cui, H. Zhou, Y. Kuang, Preparation and characterization of manganese oxide/CNT composites as supercapacitive materials, Diam. Relat. Materi. 15 (2006) 1478–1483.

[5] M.T. Kim, K.Y. Rhee, J.H. Lee, D. Hui, A.K. Lau, Property enhancement of a carbon fiber/epoxy composite by using carbon nanotubes, Compos. Part B: Eng. 42 (2011) 1257–1261

[6] S. Chuah, Z. Pan, J.G. Sanjayan, C.M. Wang, W.H. Duan, Nano reinforced cement and concrete composites and new perspective from graphene oxide, Constr. Building Mater. 73 (2014) 113–124

[7] Lee, S. H., Kang, D., Oh, I. K. (2017). Multilayered graphene-carbon nanotube-iron oxide three-dimensional heterostructure for flexible electromagnetic interference shielding film. Carbon, 111, 248-257.

[8] Y. Saez de Ibarra, J.J. Gaitero, E. Erkizia, I. Campillo, Atomic force microscopy and nanoindentation of cement pastes with nanotube dispersions. Phys. Stat. Sol. (a) 203 (2006) 1076–1081.

[9] B. Han, X. Yu, E. Kwon, A self-sensing carbon nanotube/cement composite for traffic monitoring, Nanotechnol. 20 (2009) 445501.

[10] R. Siddique, A. Mehta, Effect of carbon nanotubes on properties of cement mortars, Constr. Build. Mater. 50 (2014) 116–129.

[11] M.S. Konsta-Gdoutos, Z.S. Metaxa, S.P. Shah, Highly dispersed carbon nanotube reinforced cement based materials, Cement Concr. Res. 40 (2010) 1052–1059.

[12] E. García-Macías, A. D'Alessandro, R. Castro-Triguero, D. Pérez-Mira, F. Ubertini, Micromechanics modeling of the electrical conductivity of carbon nanotube cement-matrix composites, Compos. Part B: Eng. 108 (2017) 451–469.

[13] G.Y. Li, P.M. Wang, X. Zhao, Mechanical behavior and microstructure of cement composites incorporating surface-treated multi-walled carbon nanotubes, Carbon 43 (2005) 1239–1245.

[14] A. Chaipanich, T. Nochaiya, W. Wongkeo, P. Torkittikul, Compressive strength and microstructure of carbon nanotubes–fly ash cement composites, Mater. Sci. Eng. A, 527 (2010) 1063–1067.

[15] M.S. Morsy, S.H. Alsayed, M. Aqel, Hybrid effect of carbon nanotube and nano-clay on physico-mechanical properties of cement mortar, Constr. Build. Mater. 25 (2011) 145–149.

[16] R. Hamzaoui, A. Bennabi, S. Guessasma, R. Khelifa, N. Leklou, Optimal carbon nanotubes concentration incorporated in mortar and concrete, In Adv. Materi. Res. (Vol. 587, pp. 107-110). Trans Tech Publications.

[17] H. Choi, D. Kang, G.S. Seo, W. Chung, Effect of some parameters on the compressive strength of MWCNT-cement composites, Adv. Mater. Sci. Eng. (2015)

[18] S.J. Ha, S.T. Kang, J.H. Lee, Strength of CNT cement composites with different types of surfactants and doses, J. Kor. Inst. Struct. Maint. Insp. 19 (2015) 99–107.

[19] C.W. Nan, G. Liu, Y. Lin, M. Li, Interface effect on thermal conductivity of carbon nanotube composites, Appl. Phys. Lett. 85 (2004) 3549–3551.

[20] M.S. Liu, M.C.C. Lin, I.T. Huang, C.C. Wang, Enhancement of thermal conductivity with carbon nanotube for nanofluids, Int. Commun. Heat Mass Transf. 32 (2005)1202–1210.

[21] G.Y. Li, P.M. Wang, X. Zhao, Pressure-sensitive properties and microstructure of carbon nanotube reinforced cement composites, Cement Concr. Compos. 29 (2007) 377–382.

[22] Q. Zhang, H. Li, Experimental investigation on the ice/snow melting performance of CNFP & MWCNT/cement-based deicing system, In Proceedings of the 6th International Workshop on Advanced Smart Materials and Smart Structures Technology, Dalian, China, 2011, pp. 25–26.

[23] H.K. Kim, I.W. Nam, H.K. Lee, Enhanced effect of carbon nanotube on mechanical and electrical properties of cement composites by incorporation of silica fume, Compos. Struct. 107 (2014) 60–69.

[24] M.S. Konsta-Gdoutos, C.A. Aza, Self sensing carbon nanotube (CNT) and nanofiber (CNF) cementitious composites for real time damage assessment in smart structures, Cement Concr. Compos. 53 (2014) 162–169.

[25] H. Lee, Y.M. Song, K.J. Loh, W. Chung, Thermal response characterization and comparison of carbon nanotube-enhanced cementitious composites, Compos. Struct. 202 (2018) 1042–1050.

[26] H. Lee, D. Kang, J. Kim, K. Choi, W. Chung, Void detection of cementitious grout composite using single-walled and multi-walled carbon nanotubes, Cement Concr. Compos. 95 (2019) 237–246.

[27] J. Hone, M.C. Llaguno, N.M. Nemes, A.T. Johnson, J.E. Fischer, D.A. Walters, R.E. Smalley, Electrical and thermal transport properties of magnetically aligned single wall carbon nanotube films, Appl. Phys. Lett. 77 (2000) 666–668.

[28] H. Huang, C.H. Liu, Y. Wu, S. Fan, Aligned carbon nanotube composite films for thermal management, Adv. Mater. 17 (2005) 1652–1656.

[29] J.H. Kim, K.W. Nam, S.B. Ma, K.B. Kim, Fabrication and electrochemical properties of carbon nanotube film electrodes, Carbon, 44 (2006) 1963–1968.

[30] G.T. Pham, Y.B. Park, Z. Liang, C. Zhang, B. Wang, Processing and modeling of conductive thermoplastic/carbon nanotube films for strain sensing. Compos. Part B: Eng. 39 (2008) 209–216.

[31] J. Park, A. Lee, Y. Yim, E. Han, Electrical and thermal properties of PEDOT: PSS films doped with carbon nanotubes, Synth. Metals 161 (2011) 523–527.

[32] S.H. Jang, Y.L. Park, Carbon nanotube-reinforced smart composites for sensing freezing temperature and deicing by self-heating, Nanomater. Nanotechnol. 8 (2018) 1847980418776473.

[33] A. Sobolkina, V. Mechtcherine, V. Khavrus, D. Maier, M. Mende, M. Ritschel, A. Leonhardt, Dispersion of carbon nanotubes and its influence on the mechanical properties of the cement matrix, Cement Concr. Compos. 34 (2012) 1104–1113.

[34] A. Al-Dahawi, O. Öztürk, F. Emami, G. Yıldırım, M. Şahmaran, Effect of mixing methods on the electrical properties of cementitious composites incorporating different carbon-based materials, Construc. Build. Mater. 104 (2016)160–168.

641 [35] Al-Dahawi, A., Yıldırım, G., Öztürk, O., Şahmaran, M. (2017). Assessment of self-
642   sensing capability of Engineered Cementitious Composites within the elastic and
643   plastic ranges of cyclic flexural loading. Construction and Building Materials, 145, 1-
644   10.
645 [36] Yıldırım, G., Sarwary, M. H., Al-Dahawi, A., Öztürk, O., Anıl, Ö., Şahmaran, M.
646   (2018). Piezoresistive behavior of CF-and CNT-based reinforced concrete beams
647   subjected to static flexural loading: shear failure investigation. Construction and
648   Building Materials, 168, 266-279.
649 [37] Sarwary, M. H., Yıldırım, G., Al-Dahawi, A., Anıl, Ö., Khiavi, K. A., Toklu, K.,
650   Şahmaran M. (2019). Self-sensing of flexural damage in large-scale steel-reinforced
651   mortar beams. ACI Materials Journal, 116(4), 209-221.
652 [38] Yıldırım, G., Öztürk, O., Al-Dahawi, A., Ulu, A. A., Şahmaran, M. (2020). Self-
653   sensing capability of Engineered Cementitious Composites: Effects of aging and
654   loading conditions. Construction and Building Materials, 231, 117132.
655 [39] ASTM C109, Standard test method for compressive strength of hydraulic cement
656   mortars (Using 2-in, or 50-mm cube specimens), ASTM International (2016).
657 [40] KSL ISO 679, Methods of testing cements-determination of strength, Korean
658   Standards Association (2011).
659 [41] KS L 5201, Portland cement, Korean Standards Association (2016).
660 [42] KCS 14 20 10, Concrete, Korean Construction Specification (2016).
661 [43] ASTM C150, Standard specification for Portland cement, ASTM International (2012).
662 [44] J.G. Gonzalez, S. Gupta, K.J. Loh, Multifunctional cement composites enhanced with
663   carbon nanotube thin film interfaces, In Proceedings of the IEEE 104.8, 2016, pp. 1547-
664   1560
665 [45] S. Gupta, J.G. Gonzalez, K.J. Loh, Self-sensing concrete enabled by nano-engineered
666   cement-aggregate interfaces, Struct. Health Monit. 16.3 (2017) 309–323.
667 [46] Al-Dahawi, A., Sarwary, M. H., Öztürk, O., Yıldırım, G., Akın, A., Şahmaran, M.,
668   Lachemi, M. (2016). Electrical percolation threshold of cementitious composites
669   possessing self-sensing functionality incorporating different carbon-based materials.
670   Smart Materials and Structures, 25(10), 105005.
671 [47] Han, B., Yu, X., & Ou, J. (2010). Effect of water content on the piezoresistivity of
672   MWNT/cement composites. Journal of Materials Science, 45(14), 3714-3719.
673

674
675
676

17

Figure Captions

Figure 1 Schematics of various specimens.

Figure 2. Sample fabrication process.

Figure 3. Test setup for measuring electrical resistance and heating performance.

Figure 4. Variations in temperature upon application of voltage.

Figure 5. Thermal images of specimens after curing for 28 days.

Figure 6. Temperature–time curves.

Figure 7. Damaged MWCNT-covered film.

Figure 8. Electrical resistance with various parameters.

Figure 9. XRD patterns of various samples.

Figure 10. FE-SEM images of various samples.

Table Captions

Table 1. Parameters used for temperature measurements

Table 2. Properties of MWCNTs

Table 3. Mixing ratios of various specimens

Table 4. Results of heating tests

Table 5. Results of electrical resistance measurements

696
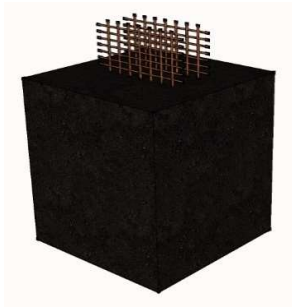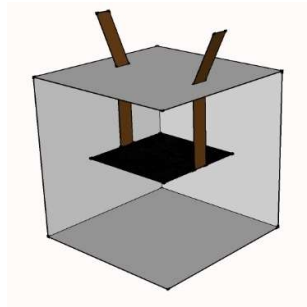
(a) MWCNT solution   (b) MWCNT films   (c) MWCNT solution and
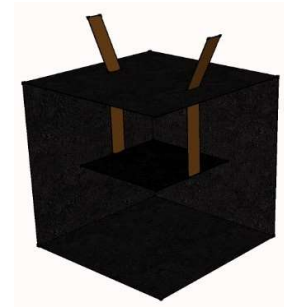
MWCNT films

697   **Fig. 1. Schematics of various specimens.**

(a)   Dispersion of MWCNTs

(b)   Mixing of cement and sand

(c)   Mixing of MWCNT dispersion (3 min)

(d)   Insertion of MWCNT films

(e)   Compaction

(f)   Insertion of thermocouple

698 **Fig. 2. Sample fabrication process.**

20
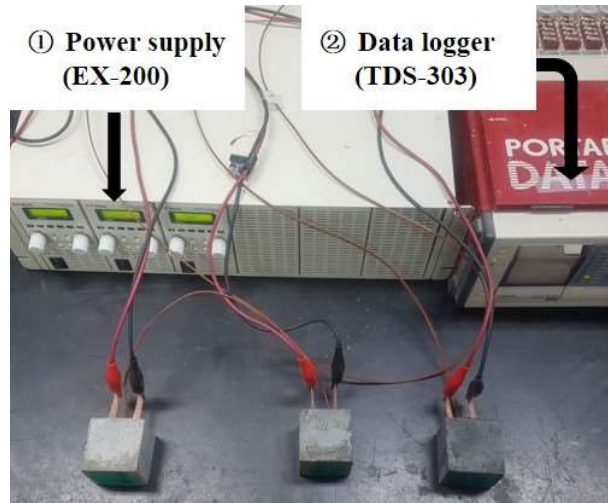
(a) Measurement of temperature upon application of voltage
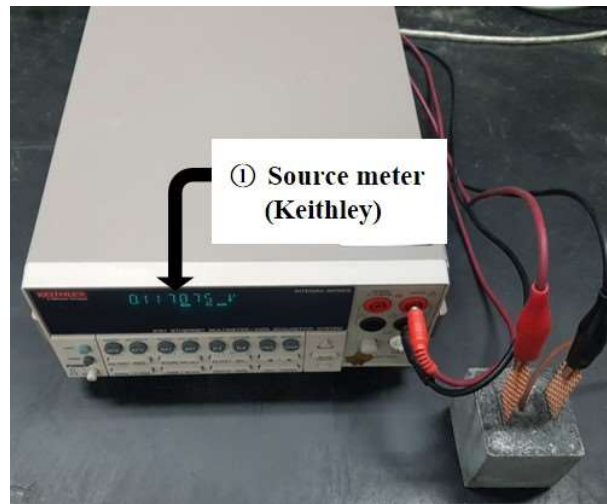
(b) Measurement of electrical resistance upon application of voltage

Fig. 3. Test setup for measuring electrical resistance and heating performance.
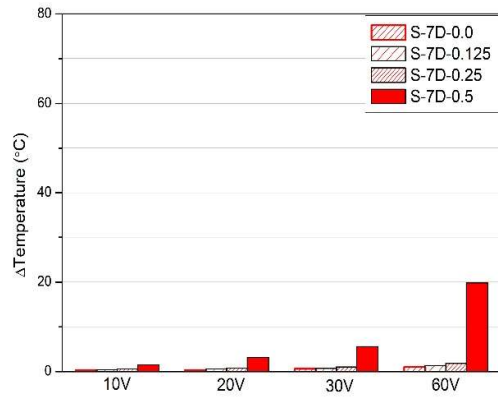
(a) MWCNT solution of 7 curing days
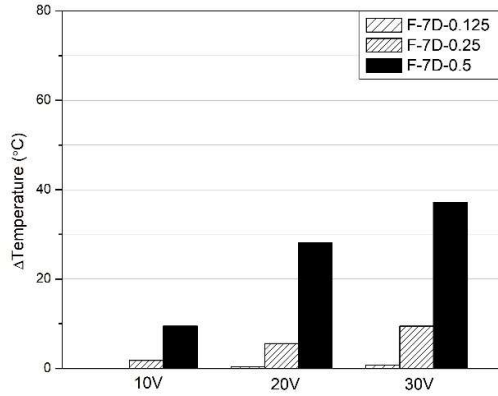
(b) MWCNT films of 7 curing days
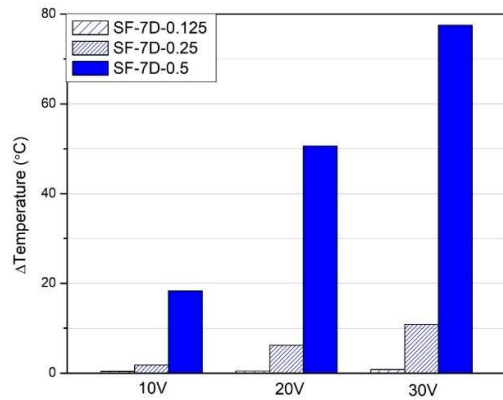
(c) MWCNT solution and MWCNT films of 7 curing days

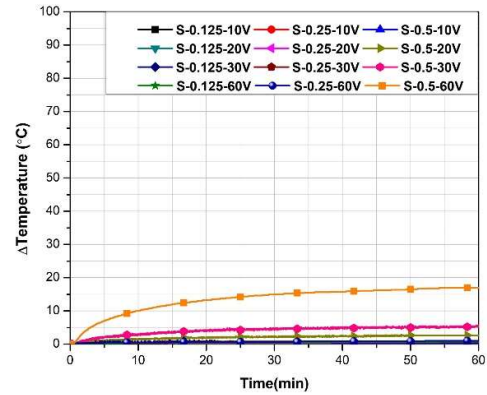**Fig. 4. Variations in temperature upon application of voltage (continue).**
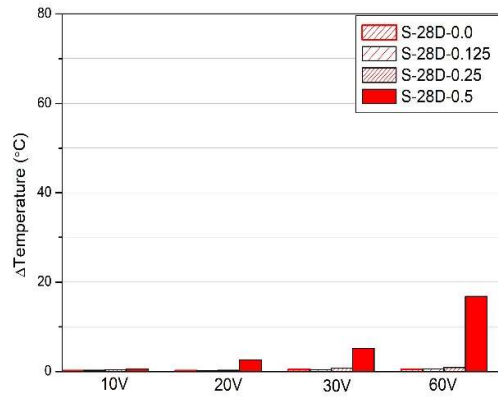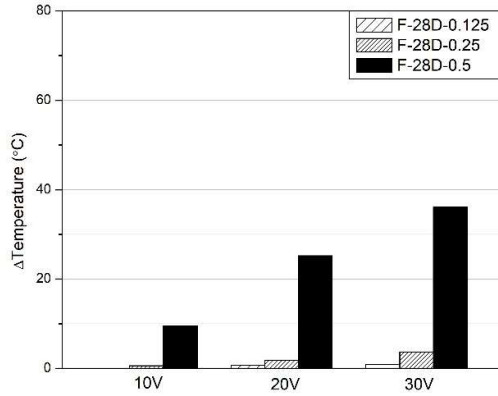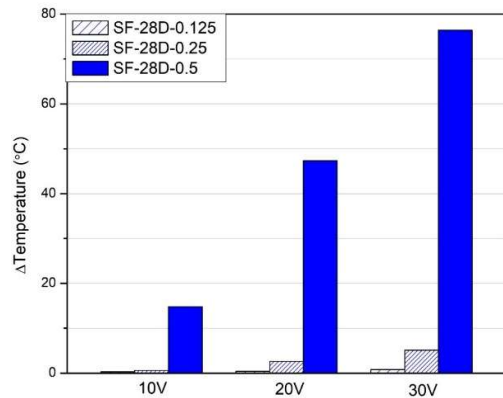
700

(d) MWCNT solution of 28 curing days

(e) MWCNT films of 28 curing days

(f) MWCNT solution and MWCNT films of 28 curing days

Fig. 4. Variations in temperature upon application of voltage.

701

(a) MWCNT solution (30 V)

(b) MWCNT solution (60 V)
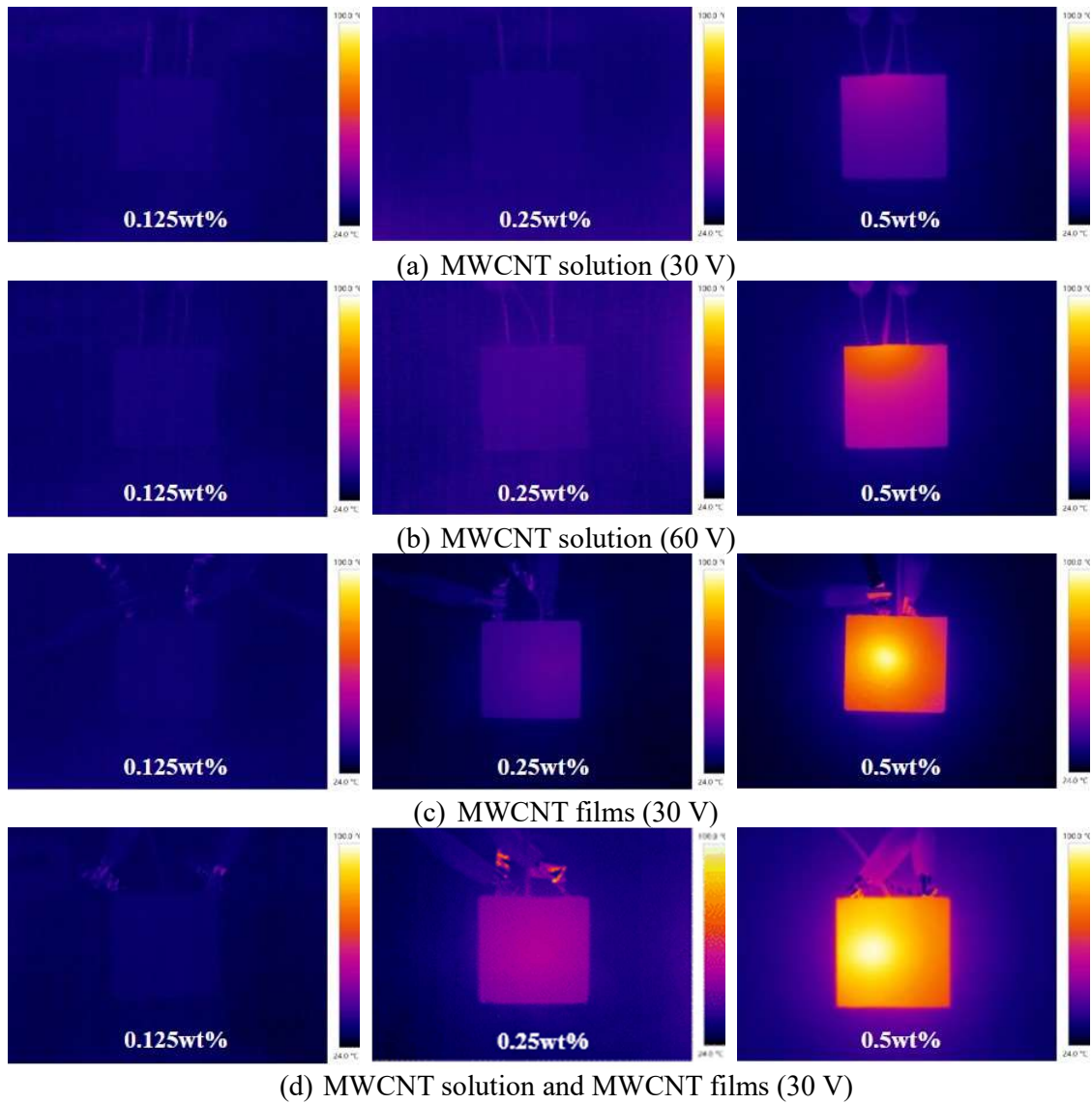
(c) MWCNT films (30 V)

(d) MWCNT solution and MWCNT films (30 V)

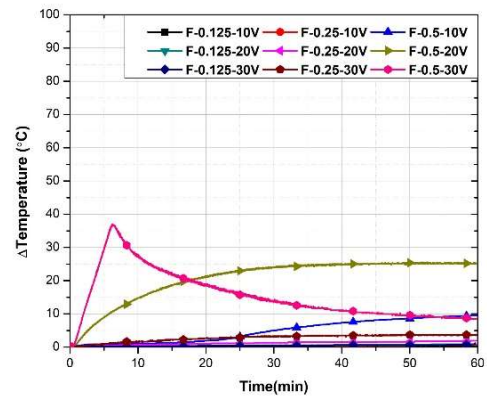**Fig. 5. Thermal images of specimens after curing for 28 days.**

702

24
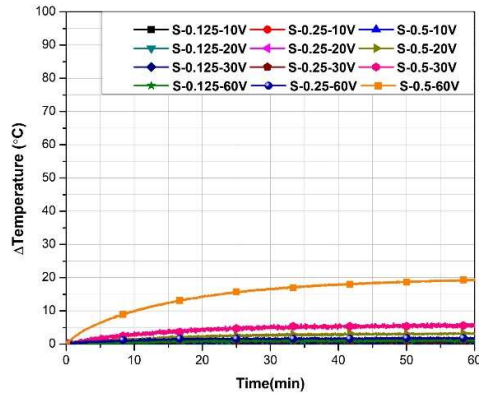
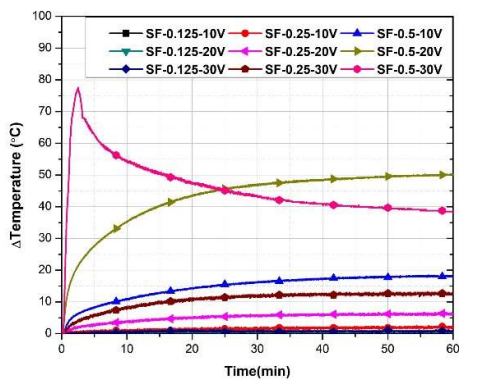(a) MWCNT solution (curing for 7 days)
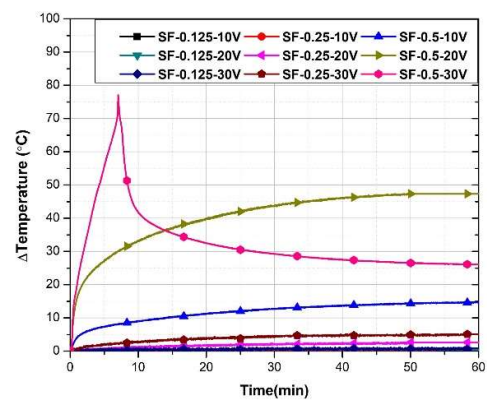
(b) MWCNT solution (curing for 28 days)
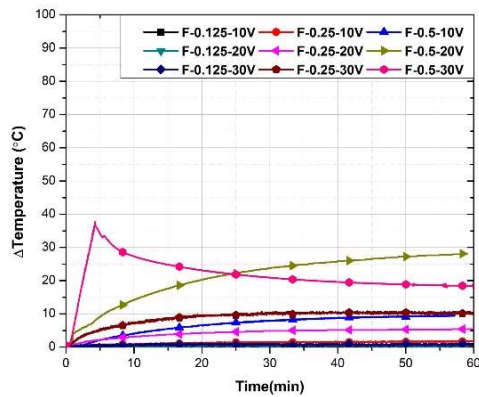
(c) MWCNT films (curing for 7 days)
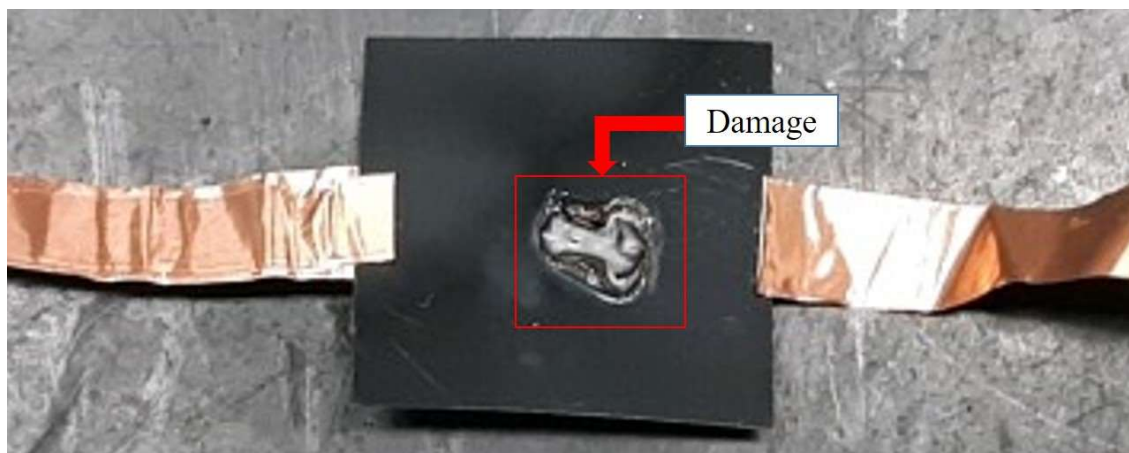
(d) MWCNT films (curing for 28 days)

(e) MWCNT solution and MWCNT films (curing for 7 days)

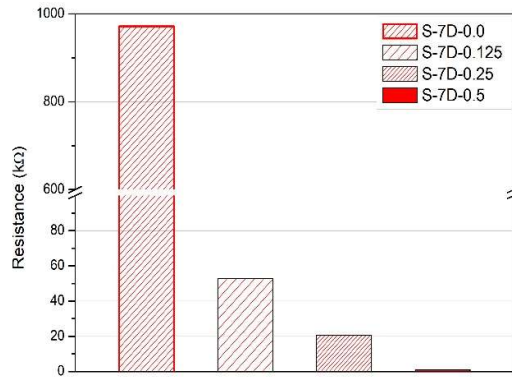(f) MWCNT solution and MWCNT films (curing for 28 days)

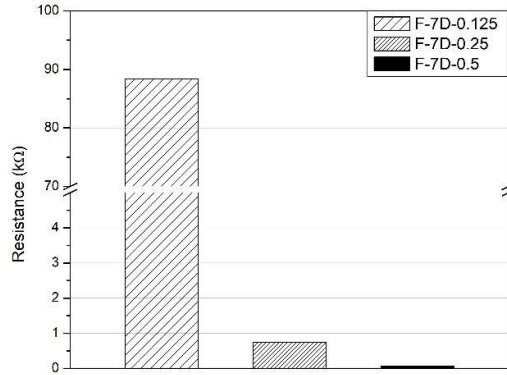703 **Fig. 6. Temperature–time curves.**

25

704
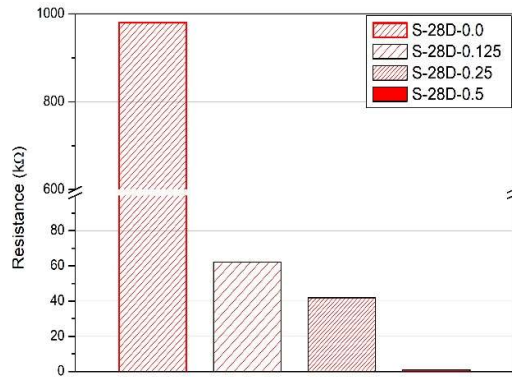
705   **Fig. 7. Damaged MWCNT-covered film.**

(a) MWCNT solution of 7 curing days

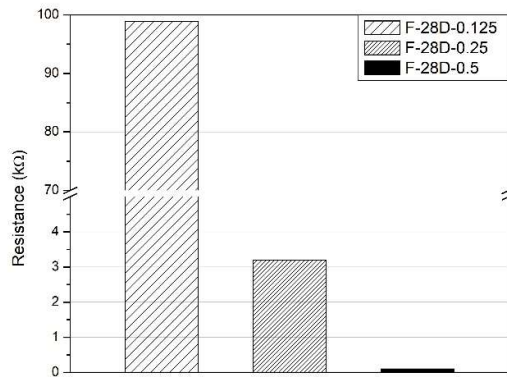(b) MWCNT films of 7 curing days

(c) MWCNT solution and MWCNT films of 7 curing days

Fig. 8. Electrical resistance for the parameter (continue).

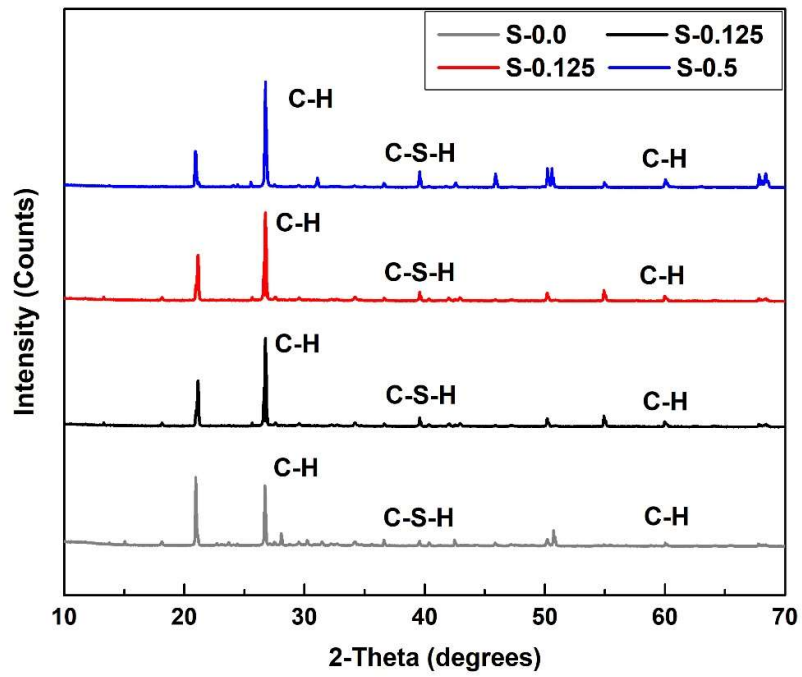706

(d) MWCNT solution of 28 curing days
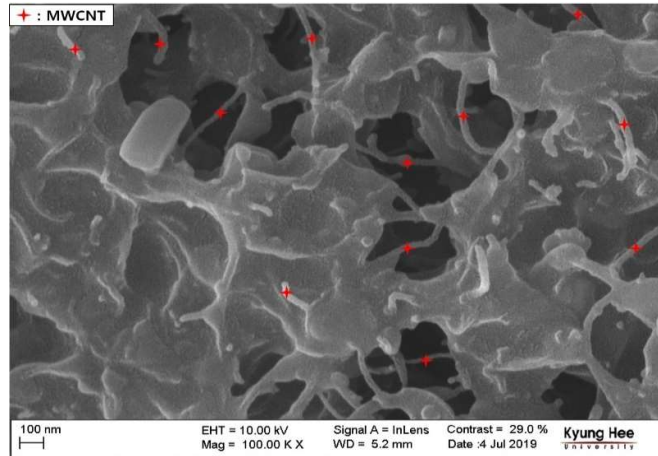

(e) MWCNT films of 28 curing days
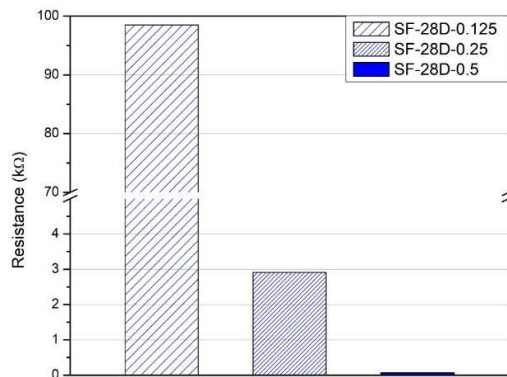
(f) MWCNT solution and MWCNT films of 28 curing days
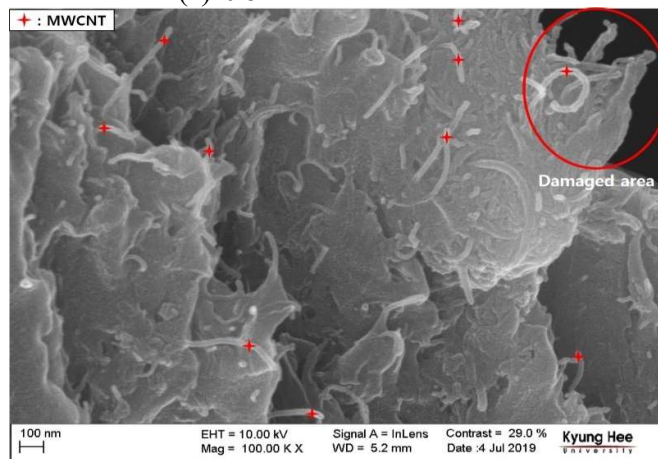**Fig. 8. Electrical resistance for the parameter.**

707

28

Fig. 9. XRD patterns of various samples.

708

(a) 0.5 wt% MWCNT solution

(b) Damaged 0.5 wt% MWCNT film
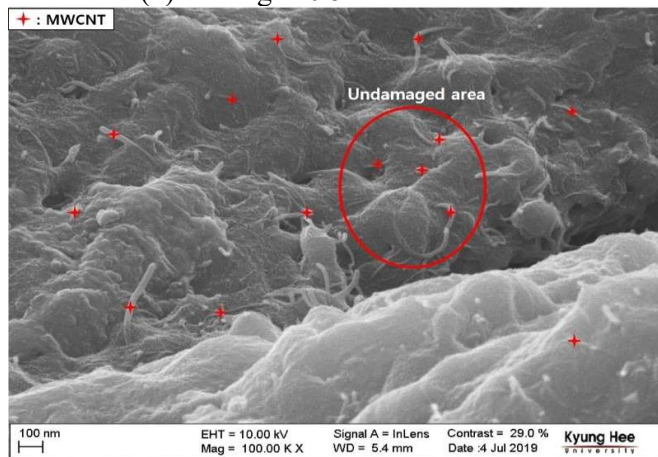
(c) Undamaged 0.5 wt% MWCNT film

Fig. 10. FE-SEM images of various samples.

709

30

Table 1. Parameters used for temperature measurements

Mixing Method	Specimen name	No. of curing days	MWCNT concentration(%)	Voltage (V)
MWCNT solution	S-7D-0.0	7	0.0	10/20/30/60
	S-7D-0.125		0.125	10/20/30/60
	S-7D-0.25		0.25	10/20/30/60
	S-7D-0.5		0.5	10/20/30/60
	S-28D-0.0	28	0.0	10/20/30/60
	S-28D-0.125		0.125	10/20/30/60
	S-28D-0.25		0.25	10/20/30/60
	S-28D-0.5		0.5	10/20/30/60
MWCNT films	F-7D-0.125	7	0.125	10/20/30
	F-7D-0.25		0.25	10/20/30
	F-7D-0.5		0.5	10/20/30
	F-28D-0.125	28	0.125	10/20/30
	F-28D-0.25		0.25	10/20/30
	F-28D-0.5		0.5	10/20/30
MWCNT solution and MWCNT films	SF-7D-0.125	7	0.125	10/20/30
	SF-7D-0.25		0.25	10/20/30
	SF-7D-0.5		0.5	10/20/30
	SF-28D-0.125	28	0.125	10/20/30
	SF-28D-0.25		0.25	10/20/30
	SF-28D-0.5		0.5	10/20/30

711

713 **Table 2. Properties of MWCNT**

Structure	Diameter : 1nm~10nm length : 100nm~1cm
Modulus of Elasticity	0.27~0.95 TPa
Tensile strength	11~63 GPa
Electrical conductivity	$0.17 \sim 2 \times 10^5$ S/cm
Thermal conductivity	3,000 W/mK
Purity	99 %
Density	1.33 g/cm

714

715

716　**Table 3. Mixing ratios of various specimens**

Name	CNTs (g)		Water/cement ratio	Water (g)	Cement (g)	Sand (g)
	MWCNT solution	MWCNT films				
S-0.0	-	-	0.5	40	80	200
S-0.125	0.05	-		40	80	200
S-0.25	0.1	-		40	80	200
S-0.5	0.2	-		40	80	200
F-0.125	-	0.05		40	80	200
F-0.25	-	0.1		40	80	200
F-0.5	-	0.2		40	80	200
SF-0.125	0.025	0.025		40	80	200
SF-0.25	0.05	0.05		40	80	200
SF-0.5	0.1	0.1		40	80	200

717

718

719   **Table 4. Results of heating tests**

Name	No. of curing days	MWCNT concentration (%)	ΔTemperature (°C)			
			10 V	20 V	30 V	60 V
S-7D-0.0	7	0.0	0.2	0.3	0.6	1.0
S-7D-0.125		0.125	0.4	0.6	0.7	1.3
S-7D-0.25		0.25	0.6	0.8	1.0	1.8
S-7D-0.5		0.5	1.5	3.2	5.6	19.8
S-28D-0.0	28	0.0	0.1	0.2	0.3	0.5
S-28D-0.125		0.125	0.1	0.2	0.4	0.6
S-28D-0.25		0.25	0.15	0.3	0.75	0.9
S-28D-0.5		0.5	0.6	2.6	5.2	16.8
F-7D-0.125	7	0.125	0.3	0.4	0.7	-
F-7D-0.25		0.25	1.8	5.6	9.5	-
F-7D-0.5		0.5	9.5	25.2	37.2	-
F-28D-0.125	28	0.125	0.4	0.7	0.9	-
F-28D-0.25		0.25	0.6	1.9	3.7	-
F-28D-0.5		0.5	9.5	28.1	36.1	-
SF-7D-0.125	7	0.125	0.2	0.5	0.8	-
SF-7D-0.25		0.25	1.8	6.2	10.9	-
SF-7D-0.5		0.5	18.3	50.6	77.5	-
SF-28D-0.125	28	0.125	0.1	0.4	0.8	-
SF-28D-0.25		0.25	0.6	2.6	5.1	-
SF-28D-0.5		0.5	14.8	47.3	76.4	-

720

34

721 **Table 5. Results of electrical resistance measurements**

Name	No. of curing days	MWCNT concentration (%)	Resistance (kΩ)
S-7D-0.0	7	0.0	972
S-7D-0.125		0.125	52.8
S-7D-0.25		0.25	20.72
S-7D-0.5		0.5	0.9
S-28D-0.0	28	0.0	980
S-28D-0.125		0.125	62.1
S-28D-0.25		0.25	25.8
S-28D-0.5		0.5	0.98
F-7D-0.125	7	0.125	88.4
F-7D-0.25		0.25	0.74
F-7D-0.5		0.5	0.075
F-28D-0.125	28	0.125	98.9
F-28D-0.25		0.25	3.2
F-28D-0.5		0.5	0.1
SF-7D-0.125	7	0.125	82.9
SF-7D-0.25		0.25	0.71
SF-7D-0.5		0.5	0.05
SF-28D-0.125	28	0.125	98.5
SF-28D-0.25		0.25	2.91
SF-28D-0.5		0.5	0.067

722

723

724   **Declarations of conflict of interest**: There are no conflicts of interest to be declared.